The voltage-gated potassium channel Kv1.3 is highly expressed on inflammatory infiltrates in multiple sclerosis brain

Horea Rus*, Carlos A. Pardo[†], Lina Hu[†], Erika Darrah[†], Cornelia Cudrici*, Teodora Niculescu*, Florin Niculescu[‡], Katharine M. Mullen[†], Rameeza Allie[†], Liping Guo[†], Heike Wulff[§], Christine Beeton[¶], Susan I. V. Judge*, Douglas A. Kerr[†], Hans-Gunther Knaus[∥], K. George Chandy[¶], and Peter A. Calabresi[†]**

[†]Department of Neurology, The Johns Hopkins University School of Medicine, Baltimore, MD 21287; *Department of Neurology, University of Maryland School of Medicine and Veterans Affairs Maryland Health Care System, Multiple Sclerosis Center of Excellence, Baltimore, MD 21201; [‡]Division of Rheumatology and Clinical Immunology, Department of Medicine, University of Maryland School of Medicine, Baltimore, MD 21201; [§]Department of Medical Pharmacology and Toxicology, University of California, Davis, CA 95616; [¶]Department of Physiology, University of California, Irvine, CA 92697; and [∥]Division for Molecular and Cellular Pharmacology, Medical University Innsbruck, 6020 Innsbruck, Austria

Multiple Sclerosis (MS) is characterized by central nervous system perivenular and parenchymal mononuclear cell infiltrates consisting of activated T cells and macrophages. We recently demonstrated that elevated expression of the voltage-gated potassium channel, Kv1.3, is a functional marker of activated effector memory T (T_{EM}) cells in experimental allergic encephalomyelitis and in myelin-specific T cells derived from the peripheral blood of patients with MS. Herein, we show that Kv1.3 is highly expressed in postmortem MS brain inflammatory infiltrates. The expression pattern revealed not only Kv1.3^{+} T cells in the perivenular infiltrate but also high expression in the parenchyma of demyelinated MS lesions and both normal appearing gray and white matter. These cells were uniformly chemokine receptor 7 negative (CCR7^{−}), consistent with an effector memory phenotype. Using double-labeling immunohistochemistry and confocal microscopy, we demonstrated colocalization of Kv1.3 with CD3, CD4, CD8, and some CD68 cells. The expression patterns mirrored in vitro experiments showing polarization of Kv1.3 to the immunological synapse. Kv1.3 was expressed in low to moderate levels on CCR7^{+} central memory T cells from cerebrospinal fluid, but, when these cells were stimulated in vitro, they rapidly became Kv1.3[high]/CCR7^{−} T_{EM}, suggesting that a subset of cerebrospinal fluid cells existed in a primed state ready to become T_{EM}. These studies provide further rationale for the use of specific Kv1.3 antagonists in MS.

lymphocytes | macrophages | cerebrospinal fluid | effector memory

Multiple sclerosis (MS) is an immune-mediated disorder in which inflammatory cells from the peripheral blood (PB) migrate to the CNS and cause demyelination and subsequent axonal degeneration (1–4). Several lines of evidence support an early role of autoreactive CD4^{+} CNS myelin-specific T cells (1, 2). In addition, there is epitope spreading such that T cell responses are directed against multiple different myelin antigens (5). Indeed, therapeutic efforts at antigen-specific therapies have not been successful or have actually worsened disease, highlighting the potential danger of antigen-specific approaches (6). The presently available agents lack specificity for autoreactive cells and have significant side effects (7, 8). There is a great need for therapies that target chronically activated memory cells involved in MS pathogenesis, but that do not cause profound immunosuppression or toxicity.

Activated T cells require high levels of intracellular calcium, which enters cells through calcium-release-activated calcium channels (CRAC) after intracellular stores are depleted of calcium (9). Membrane hyperpolarization brought about by the opening of the two lymphocyte potassium (K) channels, the voltage-gated K channel (Kv1.3), and the calcium-dependent K channel (KCa3.1, also known as IKCa1), promotes calcium entry through CRAC

channels (10). In quiescent, naive central memory T (T_{CM}) cells and effector memory T (T_{EM}) cells, Kv1.3 channels (250–400 channels per cell) are primarily responsible for the countercurrent efflux of potassium that sustains the electrochemical gradient necessary for calcium entry during the first few minutes of activation (10, 11). KCa3.1 channels are transcriptionally up-regulated in naive [CD45RA^{+}/chemokine receptor 7-positive (CCR7^{+})] and T_{CM} (CD45RA^{−}/CCR7^{+}) cells after activation (10 → 500 per cell) and become the predominant functional K^{+} channel in these cells over the ensuing days and weeks of activation (10–12). In contrast, Kv1.3 is up-regulated to 1,500–2,000 channels per cell in activated T_{EM} cells (CD45RA^{−}/CCR7^{−}) and takes over as the dominant functional K channel (11, 13). Kv1.3 blockers preferentially suppress proliferation of T_{EM} cells, whereas naive/T_{CM} cells escape inhibition by augmenting KCa3.1 expression (14). The availability of highly specific Kv1.3 inhibitors and the important role of the channel in T_{EM} cells make Kv1.3 an interesting therapeutic target in autoimmune disease in which memory T cells of multiple antigenic specificities exist at low levels in the blood and presumably become concentrated in the target organ (10, 14, 15). Indeed, several Kv1.3 antagonists have been shown to be effective in ameliorating experimental allergic encephalomyelitis (EAE) (13, 14, 16, 17).

We recently demonstrated that myelin-reactive T cells from the blood of MS patients are Kv1.3[high], suggesting they were T_{EM} cells that had undergone repeated rounds of activation in vivo. In contrast, myelin-reactive T cells from the PB of healthy controls are Kv1.3[low], consistent with a naive/T_{CM} phenotype (11). Our results corroborate reports by other investigators who have found a preponderance of chronically activated memory cells in the myelin-reactive pool in MS patients (18, 19). Here, we provide definitive evidence that Kv1.3[+] is highly expressed in the perivenular and parenchymal inflammatory infiltrates of MS brain tissue and on T cells from the cerebrospinal fluid (CSF).

Materials and Methods

Brain Tissue. Frozen brain tissue specimens were obtained at autopsy from seven patients with a definite diagnosis of MS from the Human Brain and Spinal Fluid Resource Center, Veterans Affairs West Los Angeles Health Care Center. Active lesions contained abundant infiltrates consisting of T cells and macrophages with

detectable myelin degradation products. Inflammation was restricted to the lesion margins in chronic active lesions. Regions of non-lesion white matter (NLWM) and non-lesion gray matter (NLGM) that lacked macroscopic or histological evidence of demyelination were also used. The samples were derived from patients between the ages of 30 and 51 with a mean of 44. Four additional MS brain specimens and three cases of subacute encephalitis (two with rabies and one idiopathic) were obtained at autopsy from the Brain Resource Center at The Johns Hopkins University Department of Pathology, Division of Neuropathology. Four healthy control brain samples were obtained from the Cooperative Human Tissue Network, Charlottesville, VA.

PB and CSF Cells. PB CD4$^+$ and CD8+ T cells were purified from whole blood as described (20) and stimulated with soluble anti-CD3 (1 μg/ml), anti-CD28 Abs (1 μg/ml), irradiated (3,000 rad) peripheral blood mononuclear cells, and 50 units recombinant human IL-2 (NIH Biological Resources, Bethesda), and either stained at day 3 (naive-activated) or day 10 (T$_{CM}$-activated), or maintained by restimulation with the above stimuli for 6–10 weeks (T$_{EM}$-activated). Cells were washed, spun onto glass slides, and stained as described below. Nuclei were stained with DAPI (Molecular Probes) at 1 μg/ml for 10 min and then imaged.

CSF was obtained from five MS patients and four other neurological disease controls (one ALS, one sarcoidosis, and two isolated acute transverse myelitis patients). Cells were stained immediately or placed in culture with anti-CD3 and CD28 antibodies as described below.

Cells were stained with a mouse anti-human CCR7 antibody conjugated to FITC and a rabbit anti-Kv1.3 antibody (from H.-G.K.), followed by a goat anti-rabbit IgG conjugated to Alexa Fluor 647. Z-stacks through the cells were taken by using a confocal microscope.

Antibodies. Rabbit anti-human Kv1.3 IgG were from H.-G.K. (21) and Alomone Laboratories (Jerusalem). Rabbit anti-human CD3 antibody, a monoclonal antibody to human macrophages (anti-CD68), and glial fibrillary acidic protein (GFAP) were from DAKO. The monoclonal anti-CD3 and anti-CD4 were from NovoCastra (Newcastle upon Tyne, U.K.) anti-oligodendrocyte/myelin, and phosphorylated neurofilamants from Chemicon International (Temecula, CA). The horseradish peroxidase-conjugated rabbit anti-mouse IgG, goat anti-rabbit IgG were from Jackson ImmunoResearch. The CCR7 antibody was from R & D Systems.

Immunohistochemistry on Frozen and Paraffin Sections. Cryosections were fixed in acetone containing 0.3% H$_2$O$_2$, incubated with rabbit polyclonal antibody against Kv1.3 (diluted 1/5,000), overnight at 4°C, then incubated for 1 h with goat anti-rabbit horseradish peroxidase-conjugated IgG. Specific reaction was developed by using NovaRED (Vector Laboratories). Nuclei were counterstained with Harris's hematoxylin (Sigma). Controls were prepared by immunostaining without the primary antibody, by using control isotype IgG or a blocking peptide as described (21). A similar indirect immunoperoxidase technique was used for CD3 and CD68 staining and oligodendrocytes (OLG)/myelin as described (22).

Paraffin sections were deparaffinized, heated in a pressure cooker in 10 mM citric acid (pH 6.0) for 1 min, treated with 4% normal goat serum/0.4% Triton X-100/Tris-buffered saline (TBS) for 1 h and overnight incubated with anti-Kv1.3 (1:100, Alomone Laboratories) or CD4. Sections were rinsed with TBS and incubated with biotin-conjugated secondary antibody followed by Vectastain Elite ABC and diaminobenzidine (DAB).

Immunofluorescence for Confocal Microscopy. Paraffin sections of MS brain tissue were prepared and blocked as described above. Rabbit anti-human Kv1.3 antibody and mouse monoclonals against either CD3 or CD4 were incubated at 4°C for 48 h and then

incubated overnight at 4°C in Alexa Fluor 555- and 488-conjugated secondary antibodies against the primary species antibodies (Molecular Probes). The slides were analyzed by using a Zeiss LSM 510 confocal microscope. CSF T cells were plated onto polylysine-coated coverslips, fixed with 1% paraformaldehyde (PFA), permeabilized with 0.1% Triton X-100, and incubated overnight at 4°C in blocking solution (PBS/5% goat serum/5% bovine serum-albumin/0.1% sodium azide).

Four-Color Flow Cytometry. Single-cell suspensions were prepared, stained, and analyzed on a FACSCalibur flow cytometer by using CELLQUEST software (BD Immunocytometry Systems) as described (20). All antibodies were from Pharmingen.

Electrophysiology. CSF cells were put on poly-L-lysine-coated coverslips, kept at 37°C and 5% CO$_2$ for 10 min to attach, and then patch-clamped in the whole-cell configuration as described (11, 13). Kv1.3 currents were elicited by repeated 200-ms pulses from a holding potential of −80 mV to 40 mV, applied every second to visualize the characteristic cumulative inactivation of Kv1.3, or every 30 s in experiments to measure block of ShK-F6CA (14).

Results

MS Brain Tissue. We performed immunohistochemical analysis on 20 different areas of grossly involved white matter plaques and areas of grossly uninvolved tissue from MS patients, 10 areas of healthy brain tissue, and 8 areas from brains of patients with encephalitis (Table 1 and Figs. 1 and 2). As expected, we found a predominance of CD3$^+$/CD4$^+$ T cells in the perivenular infiltrate (Fig. 1 *A* and *B Inset*). Many of these cells stained positively for Kv1.3 (Fig. 1*B*). In addition, Kv1.3$^+$ cells were highly evident in the parenchymal infiltrate of the majority of MS plaques, and the cells exhibited a membrane pattern of Kv1.3 staining (Fig. 1*C*). Serial sections through areas of intense Kv1.3 staining on lymphocytes (Fig. 1*D*)

Table 1. Expression of KV1.3 in MS lesions and control brain

Case no. (age, sex)	Lesion (no.)	Lesion type	Kv1.3 expression	
			Peri-vascular	Paren-chymal
1 (47, F)	Frontal plaques (2)	Acute	++	+++
		Non-lesion WM	++	+/++
2 (50, M)	Frontal plaques (3)	Chronic active	++	+
		Non-lesion WM	++	+
		Non-lesion GM	++	++/+++
2 (50, M)	Temporal plaques (2)	Acute	+/++	++
		Non-lesion WM	++	+
3 (50, M)	Occipital plaques (3)	Acute	++	++
		Non-lesion WM	++	++
		Non-lesion GM	+	++
4 (51, F)	Frontal plaques (2)	Acute	+/++	+/++
		Non-lesion WM	++/+++	+
5 (38, F)	Parietal plaques (3)	Chronic active	++	+/++
		Non-lesion WM	++	++
		Non-lesion GM	+/++	−
6 (38)	Occipital Plaque (3)	Acute	++	+/++
		Non-lesion WM	+	++
		Non-lesion GM	+/++	++
7 (30, F)	Frontal plaque (2)	Chronic active	+++	++
		Non-lesion WM	+/++	++
8–11	Normal (10)	Control GM	−	−
		Control WM	−	−
12–14	Encephalitis (8)	Encephalitic	− to +/++	−

F, female; M, male; WM, white matter; GM, gray matter. −, negative; +, slightly positive; ++, positive; +++, highly positive.
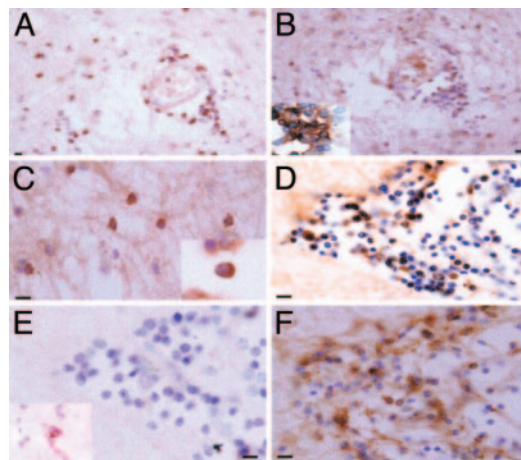
Fig. 1. Expression of Kv1.3 on inflammatory cells in MS brain. Paraffin sections were stained by indirect immunoperoxidase for Kv1.3, CD3, CD4, CCR7, and CCR5. Areas used in sectioning were from a white matter plaque. There were many perivascular inflammatory cells that stained positively for CD3 (*A*), Kv1.3 (*B*), and CD4 (*B Inset*) on consecutive sections. (*C*) Kv1.3 was also localized on inflammatory cells in the white matter parenchyma (*Inset* reveals membrane polarization of Kv1.3 staining). (*D*) Consecutive sections through another perivascular infiltrate revealed numerous Kv1.3+ inflammatory cells, which were predominantly CCR7− (*E*) (*Inset* reveals rare CCR7 positive staining), and CCR5+ (*F*). (Scale bar, 50 μm in *A* and *B* and 20 μm in *C*, *D*, *E*, and *F*.)

revealed negative CCR7 (Fig. 1*E*), but positive CCR5 staining (Fig. 1*F*) on some of the infiltrating cells. CCR7 was routinely detected on PB cytospins by using the same antibody (data not shown) and was rarely detected on perivascular cells (Fig. 1*F Inset*). These Kv1.3+ cells are therefore activated T_{EM} cells (CCR7−). We have previously shown that our staining method does not detect naive and T_{CM} (both CCR7+) in the spleen and lymph node due to the low numbers of Kv1.3 channels they express (23). There was no expression of Kv1.3 in either white matter or gray matter in normal brain tissue. We did occasionally identify a low level of Kv1.3 expression in the perivascular infiltrates from three cases of encephalitis, consistent with a CD8 memory response in cases of virally mediated encephalitis occurring over several weeks. We previously reported that CD8 memory T cells also express high levels of Kv1.3 and convert to T_{EM} faster than CD4 (11).

Interestingly, sections with grossly uninvolved white and gray matter also had areas with perivascular and parenchymal inflammatory infiltrates (Fig. 2). Many of these cells were Kv1.3+ inflammatory cells in grossly normal appearing white (Fig. 2*A*) and gray matter (Fig. 2*C*). Many of these cells were CD68+ mononuclear cells (Fig. 2*B*). No Kv1.3 staining of neurons or axonal structures was observed in gray or white matter, but, on a serial section with Kv1.3+ cells (Fig. 2*C*), we saw axonal fragmentation and neuronal swelling using a neurofilament stain, consistent with potentially tissue damaging effector immune cell activation (Fig. 2*D*). Some of the inflammatory cells had a morphology suggestive of ramified microglia (Fig. 2*E*), and, in double-labeling experiments, some but not all of the CD68+ cells also expressed Kv1.3 (Fig. 2*F*). However, consistent with the serial section analysis in Fig. 1, most Kv1.3+ cells double-labeled with CD3 (Fig. 2*G*). No background staining could be detected by using isotype control primary antibodies (Fig. 2*H*).

To better examine the localization of Kv1.3 on immune cell subsets, we examined several MS brain sections with confocal microscopy. Kv1.3 clearly localized to the cell membrane of CD3+ and CD4+ T cells in perivenular and parenchymal sections (Fig. 3). There were two patterns of staining for Kv1.3. The first was modest punctate expression of Kv1.3 in the membrane (Fig. 3*A*). The second was extensive coexpression of Kv1.3 in the membrane with CD4 (Fig. 3*B*) and in some cases CD8 (Fig. 3*C*). In some cells, there
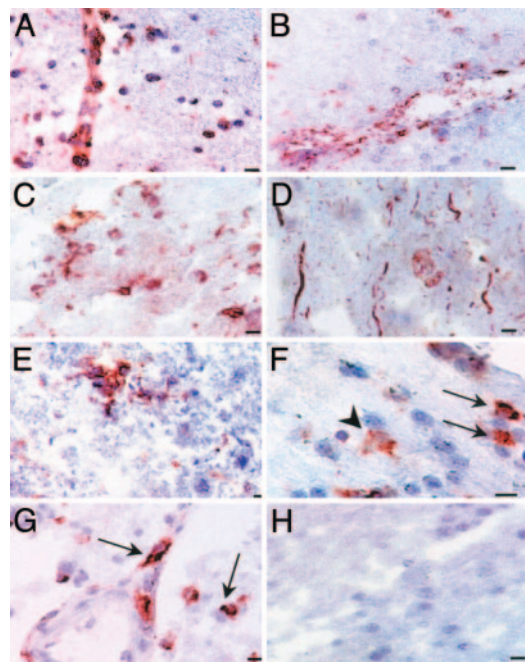

Fig. 2. Tissue expression of Kv1.3 in normal appearing white and gray matter. MS brain cryostat sections that were grossly uninvolved were examined for Kv1.3 expression. (*A*) Kv1.3 deposits were found on perivascular and parenchymal inflammatory cells in the normal appearing white matter. (*B*) Many of these cells stained positively for CD68. (*C*) Kv1.3 staining was also seen on parenchymal cells in the gray matter. (*D*) Phosphorylated neurofilament staining showed axonal fragmentation and swelling in a normal appearing gray matter area, which was a consecutive section for the Kv1.3 staining seen only on inflammatory cells in *C*. (*E*) Some of the cells were branched process bearing cells with an appearance suggestive of microglia. (*F*) Double labeling identified some Kv1.3+ cells as CD68+ cells (arrows red-Kv1.3, dark brown CD68); not all CD68 cells expressed Kv1.3 (arrowheads). (*G*) Double labeling with CD3 (dark brown) and Kv1.3 (red) was also clearly seen. Not all Kv1.3-expressing cells are CD68 positive. (*H*) Control of the immunoperoxidase reaction. (Scale bar, 20 μm in *A*, *B*, *D*, *G*, and *H*; 50 μm in *C* and *F*; and 10 μm in *E*.)

was marked colocalization of Kv1.3 and CD3 (Fig. 3*D*). The latter pattern was rarer, consistent with the fact that the majority of T cells found in postmortem tissue have not been recently activated even in sites of chronic active inflammation. Extensive colocalization of CD4 and Kv1.3 was seen on acutely activated CD4+/CCR7− T_{EM} cells (24–96 h) (Fig. 3 *F* and *G*) resembling the MS brain pattern in (Fig. 3*D*). Activated CD8 T_{EM} cells also stained positively for Kv1.3 and exhibited extensive CD8 and Kv1.3 colocalization (Fig. 3*I*). In contrast, *in vitro* polyclonally stimulated CD4+ naive/T_{CM} cells (7 days after stimulation) and *in vitro*-activated naive CD8+ T cells did not exhibit visible Kv1.3 staining (Fig. 3 *E* and *H*). These data correlate well with known Kv1.3 electrophysiological currents that can be detected in resting and activated CD4+ and CD8+ naive T_{CM} and T_{EM} cells (11).

CSF Cells. We also examined CSF cell samples derived from MS patients and controls. The cells were predominantly (90–95%) lymphocytes (CD4 > CD8) of the T_{CM} phenotype (CD45RA−/CCR7+) (Fig. 4*A*). Because our data and several previous reports have suggested that CSF cells from MS patients are primed memory cells that express high levels of CXCR3 and have effector functions, we postulated that these cells would rapidly convert into T_{EM} after stimulation (24–27). Indeed, upon stimulation *in vitro*, we found that the CSF cells from MS patients rapidly became CCR7− at day 7 and maintained this phenotype at day 14 (Fig. 4 *B* and *C*). In contrast, CSF cells from noninflammatory neurological controls
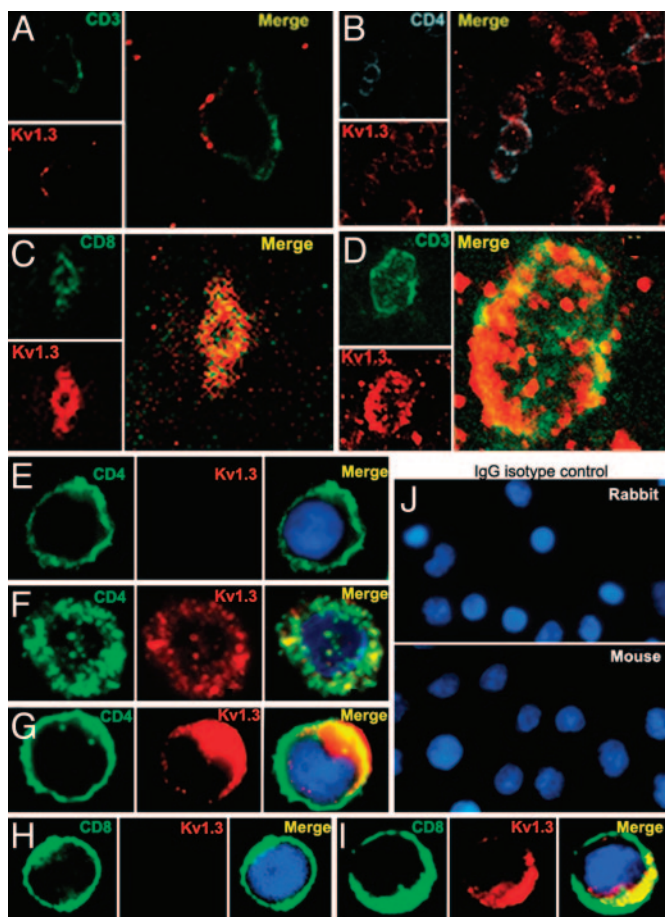
Fig. 3. Confocal microscopy of Kv1.3 and CD3/CD4 in MS brain tissue. Confocal microscopic images of 20-μm floating sections of postmortem MS brain tissue. (*A* and *B*) Parenchymal infiltrate with positive CD3 and punctate Kv1.3 staining in the membrane. (*C*) A cluster of lymphocytes stained positively for Kv1.3 and CD4, as well as occasional CD8 (*Inset*). (*D*) CD3$^+$ cells showed extensive Kv1.3 and CD3 colocalization in the membrane. Immunofluorescent staining of PB-derived T cells concentrated on a slide by cytospin showed membrane patterns of staining of CD4, CD8, and Kv1.3. (*E*) Day 7-activated naive and T$_{CM}$ are CD4$^+$, CCR7$^+$ (data not shown) and Kv1.3$^-$. (*F*) Chronically stimulated resting T$_{EM}$ were CD4$^+$, CCR7$^-$ (data not shown) and expressed Kv1.3 in the membrane but with minimal colocalization with CD4. (*G*) T$_{EM}$ that had been recently activated expressed increased amounts of Kv1.3 and demonstrated more colocalization with CD4 similar to the brain tissue lymphocyte in *D*. (*H*) Naive CD8$^+$ T cells expressed no Kv1.3 but, when chronically stimulated and activated (*I*), exhibited intense Kv1.3 expression and colocalization with CD8. (*J*) Isotype controls using nonspecific rabbit primary antibody followed by usual secondary label and with primary rabbit anti-human and nonspecific labeled mouse anti-rabbit secondary antibody showed no background staining.

were predominantly T$_{CM}$ and retained the T$_{CM}$ phenotype after stimulation, suggesting that these cells are in an earlier state of differentiation (Fig. 4 *D* and *E*). The very low frequency of these cells made it difficult to track them for longer periods of time. CD4$^+$ T cells from the PB of healthy controls or MS patients were either of the naive or T$_{CM}$ phenotype but, upon identical stimulation for 7 and 14 days, did not convert to T$_{EM}$ cells (Fig. 4 *F–H*).

We studied Kv1.3 currents in *ex vivo* CSF cells from five patients with MS. Cells from three patients were examined immediately after isolation, whereas samples from two others were activated for 7–14 days and then patch-clamped. The K$^+$ currents in these cells displayed biophysical and pharmacological properties closely resembling those of Kv1.3. Depolarizing pulses of 500-ms duration applied from a holding potential of −80 mV to various voltages

induced a family of outward K$^+$ currents (Fig. 4*I*). From these data, we generated a conductance–voltage curve (Fig. 4*K*) and calculated $V_{1/2}$ to be −28 mV ($V_{1/2}$ for Kv1.3 = −29 to −33 mV). Repeated depolarizing pulses applied every second resulted in a decrease in maximal current amplitude with each successive pulse (Fig. 4*L*), which is characteristic of Kv1.3. The activation (3 ± 0.3 mV, $n = 5$) and inactivation (280 ± 15 ms, $n = 5$) time constants at 40 mV were also constant with the current being Kv1.3. The current was blocked by the most selective Kv1.3 inhibitor currently known, ShK(L5), with a concentration dependence identical to Kv1.3 (Fig. 4 *M* and *N*).

The Kv1.3 channel numbers per T cell are shown in Fig. 4*I*. CSF sample 1 expressed the Kv1.3^{high} pattern of activated T$_{EM}$ effectors (≈1,300 Kv1.3 per cell), whereas cells from CSF samples 2 and 3 exhibited the Kv1.3^{low} pattern of activated naive/T$_{CM}$ cells (≈600 Kv1.3 per cell). Due to the small numbers of cells in these CSF samples, we were unable to assess the Kv1.3 channel numbers after activation in samples 1–3. Instead, CSF samples 4 and 5 were activated for 7–14 days with anti-CD3/28 beads and then patch-clamped. Consistent with the flow cytometry data (Fig. 4 *A–H*), these cells acquired the Kv1.3^{high} pattern of T$_{EM}$ effectors after activation (Fig. 4*I*). In contrast, anti-CD3-activated PB T cells from MS patients expressed the Kv1.3^{low} pattern of activated naive/T$_{CM}$ cells (Fig. 4*I*), similar to PB T cells from healthy controls; myelin-specific T cells in the blood are at such low frequency that the chances of patching these cells is very low.

To confirm the patch-clamp data, we stained cells from CSF samples 3 and 5 with antibodies specific for CCR7 and Kv1.3 and then visualized the stained cells by confocal microscopy. Sample 3 with Kv1.3^{low} cells stained strongly for CCR7 but was negative for Kv1.3 (Fig. 4*O*), consistent with these cells being naive/T$_{CM}$ cells. In contrast, sample 5 with Kv1.3^{high} cells stained strongly for Kv1.3 and weakly for CCR7 (Fig. 4*O*). Sample 3 was CCR7$^+$Kv1.3^{low} whereas sample 5 was Kv1.3^{high}CCR7^{low}, confirming the patch-clamp data. The staining intensity is presented in Fig. 4*P*.

To ensure that the channel protein was in the membrane, a set of Z-stack images were captured and analyzed (Fig. 4*Q*); these images show that Kv1.3 is in the membrane in CSF T cells. Taken together, these data indicate that T cells in the CSF of MS patients rapidly transition into Kv1.3^{high} CCR7$^-$-activated T$_{EM}$ effectors upon stimulation.

Discussion

We have observed extensive positive staining for the voltage-gated potassium channel Kv1.3 on CD3$^+$ lymphocytes in MS brain tissue. Most of these Kv1.3$^+$ cells were CCR7$^-$, which strongly suggests that the majority of the inflammatory infiltrate in MS brain are activated T$_{EM}$ cells that have undergone repeated antigen stimulation *in vivo* during the course of disease. Our finding of Kv1.3$^+$-activated T$_{EM}$ cells in MS brain tissue infiltrates and of Kv1.3^{high}-activated T$_{EM}$ cells in CSF from MS patients is a demonstration of elevated Kv1.3 expression in lymphocytes in target autoimmune tissue. These results extend our recent demonstration that myelin-reactive T cells in the PB of MS patients are Kv1.3^{high}-activated T$_{EM}$ cells (11). Our findings in MS are distinctly different from EAE in mice, in which only a small percentage of the inflammatory infiltrate are antigen-specific cells and the majority of the cells are likely to have been nonspecifically recruited (28). The relative ease of targeting nonspecifically recruited cells that have many early activation markers could explain why EAE is more amenable to therapeutic interventions than the human disease MS, in which differentiated T$_{EM}$ cells predominate in the brain.

The loss of CCR7, a lymph node-homing receptor, seems to be a critical switch that correlates with the up-regulation of the T helper 1-associated chemokine receptor CCR5 and allows T cells to migrate to tissue sites of inflammation and perform effector activities (29). Potassium channels play a critical role in maintaining the electrochemical gradient required for sustained calcium entry

Fig. 4. Immunofluorescence and electrophysiology of peripheral and CSF T cells. FACS plots revealed staining patterns of CCR7 vs. CD45RA. (*A*) CD4-gated MS-derived CSF cells revealed a predominantly T_{CM} phenotype immediately *ex vivo*, but with rapid conversion to short-lived T_{EM} after 7 and 14 days of stimulation using anti-CD3/CD28 coated beads (*B* and *C*). By comparison, negatively sorted CSF derived from noninflammatory neurological controls showed CD4$^+$ cells that were predominantly T_{CM} (*D*) and remained T_{CM} at day 7 despite identical manner of stimulation (*E*). (*F–H*) CD4 cells derived from PB were predominantly T_{CM} and naive phenotype (*F*), and maintained high levels of CCR7 even after 7 and 14 days of stimulation using anti-CD3/CD28 coated beads (*G* and *H*). (*I*) Single cell patch-clamp analysis of MS-derived CSF cells revealed high Kv1.3 channel numbers per cell; mean channel number per cell was 1,082 ± 489 (mean ± SEM, n = 28). Shown for comparison on the right are mean Kv1.3 channel numbers from activated PB T cells from three MS patients (n = 32), and from 10 healthy controls (n = 33). (*J* and *K*) Family of currents. The test potential was changed from −60 to 60 mV in 10-mV increments every 30 s ($V_{1/2}$ = −28 mV). (*L*) The current in CSF cells exhibited the characteristic use-dependence of Kv1.3 when 200-ms pulses were applied every second to 40 mV. (*M* and *N*) Pharmacological blockade with the potent and selective Kv1.3 inhibitor ShK(L5) (14) confirmed that the current is carried by Kv1.3. (*O*) Representative images of CSF resting (top) or activated (bottom) T cells stained with anti-Kv1.3 and CCR7 Abs. (*P*) Staining intensities for Kv1.3 and CCR7 in resting and activated CSF T cells. (*Q*) Z-stack of confocal images through an activated CSF T cell.

in the time frame required for activation and effector function (10). We previously reported that activated T_{EM} cells have a 4- to 6-fold elevation in the numbers of functional Kv1.3 channels expressed per cell compared with activated naive/T_{CM} cells (11). This enhanced Kv1.3 expression is likely to promote calcium signaling necessary for

activated memory cells to perform their effector functions. Blockade of the Kv1.3 channel suppresses antigen-driven proliferation and cytokine production by these cells, and selective Kv1.3 blockers ameliorate EAE in rats induced by the adoptive transfer of myelin-specific activated T_{EM} cells (13, 14, 16).

Our discovery that CCR7$^+$ CSF lymphoblasts have slightly increased Kv1.3 channels on their membrane, but are primed to rapidly become Kv1.3^{high} T$_{EM}$ has important implications in understanding CNS recruitment. These data are consistent with a recent report by another group (30) in which CSF cells were CCR7$^+$ but parenchymal cells were CCR7$^-$. We considered the possibility that CCR7 expression might reflect their activation state because we and others have reported that CCR7 is transiently up-regulated on T helper 1 cells during early activation (20, 31). However, our MS-derived CSF cells rapidly became CCR7$^-$ T$_{EM}$ within a week of strong TCR engagement and costimulation *in vitro*, and their Kv1.3 channel number increased dramatically, unlike PBL or control CSF cells. We have never seen this rapid conversion of T$_{CM}$ to T$_{EM}$ while generating antigen-specific T cell clones *in vitro*, which suggests that the MS CSF cells are in a primed state, but require a second strong signal within the CNS to allow their conversion to effector cells that are then retained within the parenchyma. The concept of a primed CCR7$^+$/CXCR3$^+$ cell, such as is the phenotype of MS CSF cells, was recently described *in vitro* and is considered the precursor of T helper 1 cells (32, 33). The requirement for a strong reactivating signal at the blood–brain barrier may be an important regulatory mechanism to prevent damaging effector cell infiltration when not needed.

The expression of Kv1.3 on a number of macrophages and microglial cells was of additional interest. Several groups (34–40) have described Kv1.3 expression on macrophages and microglia *in vitro* or in rodent tissues, but never in human brain tissue. Kv1.3 channels are required only for the later stages of proliferation of rodent microglia, whereas Kv1.5 channels are necessary during the early stages (36). Other studies suggest that Kv1.3 channels, together with Kir2.1, Kv1.5, KCa3.1, and BK$_{Ca}$ channels, modulate

macrophage and microglia function (35, 38, 41–43). Kv1.3 blockers may therefore have effects on chronically activated T$_{EM}$ cells, and may also partially influence the function of microglia and brain macrophages.

In summary, these pathological findings, in conjunction with our previous *in vitro* report, suggest that Kv1.3 is a functional marker of activated T$_{EM}$ cells, and that these are the predominant lymphocyte cell type in MS inflammatory brain infiltrates. The therapeutic appeal of Kv1.3 is that it does not require knowledge of antigen specificity, which may be critical in diseases where epitope spreading occurs. Further, the presence of elevated Kv1.3 levels on both CD4$^+$ and CD8$^+$ activated T$_{EM}$ cells suggests that Kv1.3 antagonists could target both CD4 and CD8 T$_{EM}$ functions such as the release of the destructive protease granzyme B, which has been implicated in mediating direct cytolytic damage in progressive MS (44, 45). The availability of Kv1.3-specific antagonists with demonstrated efficacy *in vitro* and in Lewis rat adoptive EAE makes Kv1.3 an attractive therapeutic target in MS, and possibly other autoimmune diseases (10, 11, 14).

1. Hafler, D. A. (2004) *J. Clin. Invest.* **113,** 788–794.
2. Sospedra, M. & Martin, R. (2004) *Annu. Rev. Immunol.* **23,** 683–747.
3. Lassmann, H. (2004) *J. Neurol.* **251,** Suppl. 4, IV2–IV5.
4. Trapp, B. D., Peterson, J., Ransohoff, R. M., Rudick, R., Mork, S. & Bo, L. (1998) *New Engl. J. Med.* **338,** 278–285.
5. Vanderlugt, C. L. & Miller, S. D. (2002) *Nat. Rev. Immunol.* **2,** 85–95.
6. Bielekova, B., Goodwin, B., Richert, N., Cortese, I., Kondo, T., Afshar, G., Gran, B., Eaton, J., Antel, J., Frank, J. A., *et al.* (2000) *Nat. Med.* **6,** 1167–1175.
7. Dhib-Jalbut, S. (2002) *Neurology* **58,** S3–S9.
8. Yong, V. W. (2002) *Neurology* **59,** 802–808.
9. Cahalan, M. D., Wulff, H. & Chandy, K. G. (2001) *J. Clin. Immunol.* **21,** 235–252.
10. Chandy, K. G., Wulff, H., Beeton, C., Pennington, M., Gutman, G. A. & Cahalan, M. D. (2004) *Trends Pharmacol. Sci.* **25,** 280–289.
11. Wulff, H., Calabresi, P. A., Allie, R., Yun, S. H., Pennington, M., Beeton, C. & Chandy, K. G. (2003) *J. Clin. Invest.* **111,** 1703–1713.
12. Ghanshani, S., Wulff, H., Miller, M. J., Rohm, H., Neben, A., Gutman, G. A., Cahalan, M. D. & Chandy, K. G. (2000) *J. Biol. Chem.* **275,** 37137–37149.
13. Beeton, C., Barbaria, J., Giraud, P., Devaux, J., Benoliel, A. M., Gola, M., Sabatier, J. M., Bernard, D., Crest, M. & Beraud, E. (2001) *J. Immunol.* **166,** 936–944.
14. Beeton, C., Pennington, M. W., Wulff, H., Singh, S., Nugent, D., Crossley, G., Khaytin, I., Calabresi, P. A., Chen, C. Y., Gutman, G. A. & Chandy, K. G. (2005) *Mol. Pharmacol.* **67,** 1369–1386.
15. Wulff, H., Beeton, C. & Chandy, K. G. (2003) *Curr. Opin. Drug. Discov. Devel.* **6,** 640–647.
16. Beeton, C., Wulff, H., Barbaria, J., Clot-Faybesse, O., Pennington, M., Bernard, D., Cahalan, M. D., Chandy, K. G. & Beraud, E. (2001) *Proc. Natl. Acad. Sci. USA* **98,** 13942–13947.
17. Judge, S. I., Yeh, J. Z., Mannie, M. D., Pope Seifert, L. & Paterson, P. Y. (1997) *J. Biomed. Sci.* **4,** 169–178.
18. Lovett-Racke, A. E., Trotter J. L., Lauber J., Perrin P. J., June C. H., Racke M. K. (1998) *J. Clin. Invest.* **101,** 725–730.
19. Scholz, C., Patton, K. T., Anderson, D. E., Freeman, G. J. & Hafler, D. A. (1998) *J. Immunol.* **160,** 1532–1538.
20. Calabresi, P. A., Allie, R., Mullen, K. M., Yun, S. H., Georgantas, R. W., 3rd, & Whartenby, K. A. (2003) *J. Neuroimmunol.* **139,** 58–65.
21. Koch, R. O., Wanner, S. G., Koschak, A., Hanner, M., Schwarzer, C., Kaczorowski, G. J., Slaughter, R. S., Garcia, M. L. & Knaus, H. G. (1997) *J. Biol. Chem.* **272,** 27577–27581.
22. Niculescu, T., Weerth, S., Niculescu, F., Cudrici, C., Rus, V., Raine, C. S., Shin, M. L. & Rus, H. (2004) *J. Immunol.* **172,** 5702–5706.
23. Wulff, H., Knaus, H. G., Pennington, M. & Chandy, K. G. (2004) *J. Immunol.* **173,** 776–786.
24. Calabresi, P. A., Tranquill, L. R., McFarland, H. F. & Cowan, E. P. (1998) *J. Neuroimmunol.* **89,** 198–205.
25. Sorensen, T. L., Tani, M., Jensen, J., Pierce, V., Lucchinetti, C., Folcik, V. A., Qin, S., Rottman, J., Sellebjerg, F., Strieter, R. M., *et al.* (1999) *J. Clin. Invest.* **103,** 807–815.
26. Chofflon, M., Gonzalez, V., Weiner, H. L. & Hafler, D. A. (1989) *Eur. J. Immunol.* **19,** 1791–1795.
27. Rieckmann, P., Albrecht, M., Ehrenreich, H., Weber, T. & Michel, U. (1995) *Res. Exp. Med. (Berl.)* **195,** 17–29.
28. Cross, A. H., Cannella, B., Brosnan, C. F. & Raine, C. S. (1990) *Lab. Invest.* **63,** 162–170.
29. Sallusto, F., Kremmer, E., Palermo, B., Hoy, A., Ponath, P., Qin, S., Forster, R., Lipp, M. & Lanzavecchia, A. (1999) *Eur. J. Immunol.* **29,** 2037–2045.
30. Kivisakk, P., Mahad, D. J., Callahan, M. K., Sikora, K., Trebst, C., Tucky, B., Wujek, J., Ravid, R., Staugaitis, S. M., Lassmann, H. & Ransohoff, R. M. (2004) *Ann. Neurol.* **55,** 627–638.
31. Randolph, D. A., Huang, G., Carruthers, C. J., Bromley, L. E. & Chaplin, D. D. (1999) *Science* **286,** 2159–2162.
32. Rivino, L., Messi, M., Jarrossay, D., Lanzavecchia, A., Sallusto, F. & Geginat, J. (2004) *J. Exp. Med.* **200,** 725–735.
33. Sorensen, T. L., Trebst, C., Kivisakk, P., Klaege, K. L., Majmudar, A., Ravid, R., Lassmann, H., Olsen, D. B., Strieter, R. M., Ransohoff, R. M. & Sellebjerg, F. (2002) *J. Neuroimmunol.* **127,** 59–68.
34. Ypey, D. L. & Clapham, D. E. (1984) *Proc. Natl. Acad. Sci. USA* **81,** 3083–3087.
35. Gallin, E. K. (1984) *Biophys. J.* **46,** 821–825.
36. Kotecha, S. A. & Schlichter, L. C. (1999) *J. Neurosci.* **19,** 10680–10693.
37. DeCoursey, T. E., Kim, S. Y., Silver, M. R. & Quandt, F. N. (1996) *J. Membr. Biol.* **152,** 141–157.
38. Vicente, R., Escalada, A., Coma, M., Fuster, G., Sanchez-Tillo, E., Lopez-Iglesias, C., Soler, C., Solsona, C., Celada, A. & Felipe, A. (2003) *J. Biol. Chem.* **278,** 46307–46320.
39. Mackenzie, A. B., Chirakkal, H. & North, R. A. (2003) *Am. J. Physiol. Lung Cell Mol. Physiol.* **285,** L862–L868.
40. Schilling, T., Quandt, F. N., Cherny, V. V., Zhou, W., Heinemann, U., Decoursey, T. E. & Eder, C. (2000) *Am. J. Physiol. Cell Physiol.* **279,** C1123–C1134.
41. Blunck, R., Scheel, O., Muller, M., Brandenburg, K., Seitzer, U. & Seydel, U. (2001) *J. Immunol.* **166,** 1009–1015.
42. Ahluwalia, J., Tinker, A., Clapp, L. H., Duchen, M. R., Abramov, A. Y., Pope, S., Nobles, M. & Segal, A. W. (2004) *Nature* **427,** 853–858.
43. Khanna, R., Roy, L., Zhu, X. & Schlichter, L. C. (2001) *Am. J. Physiol. Cell Physiol.* **280,** C796–C806.
44. Neumann, H., Medana, I. M., Bauer, J. & Lassmann, H. (2002) *Trends Neurosci.* **25,** 313–319.
45. Hoftberger, R., Aboul-Enein, F., Brueck, W., Lucchinetti, C., Rodriguez, M., Schmidbauer, M., Jellinger, K. & Lassmann, H. (2004) *Brain Pathol.* **14,** 43–50.

NEUROSCIENCE